Int. J. Heat Mass Transfer. Vol. 28, No. 6, pp. 1165–1171, 1985
Printed in Great Britain

0017-9310/85 $3.00+0.00
Pergamon Press Ltd.

Similarity properties in the problem of flow from a supersonic source past a spherical bluntness

Yu. P. GOLOVACHOV
A. F. Ioffe Physical–Technical Institute of the USSR Academy of Sciences, Leningrad, U.S.S.R.

(*Received* 16 *April* 1984)

Abstract—The steady-state perfect gas flow from a supersonic spherical source past a spherical bluntness is considered. Based on numerical solutions to the nonviscous gas equations, boundary-layer and Navier–Stokes equations, universal relations for the heat transfer and drag parameters are constructed that apply in a wide range of Mach and Reynolds numbers for various free-stream uniformities.

INTRODUCTION

At the present time aerodynamic investigations widely employ facilities in which the flow of supersonic under-expanded jets around bodies occurs. As a simplest mathematical model approximately describing the flow field in a supersonic under-expanded jet one may consider the flow from a supersonic source.

Supersonic source flows past blunt bodies have been treated theoretically in a number of studies [1–3]. Within the framework of the nonviscous gas model, the effect of the nonuniform character of flow on the shock-layer and pressure distribution over the body surface was investigated. Similar behaviour of flow parameters in the neighbourhood of the forward stagnation point was found when the angle coordinate is scaled in accordance with free-stream nonuniformity. Based on the thin shock-layer and boundary-layer models, an analytical approximation was suggested for heat flux distribution over the sphere surface at hypersonic free-stream velocities [4]. The effect of nonuniformity on the properties of flow past blunt bodies at moderate Reynolds numbers was analysed in study [5] where numerical solutions of full Navier–Stokes equations were obtained.

In the present paper, based on numerical solutions to the nonviscous gas and boundary-layer equation and on the results obtained earlier [5], universal relations are derived to determine the shape of the bow shock wave, pressure, shear stress, and heat flux on the sphere surface at Reynolds numbers $Re_s \gtrsim 50$.

STATEMENT OF THE PROBLEM AND NUMERICAL SOLUTIONS

The centres of a sphere, immersed in a flow, and of a spherical source are separated from each other by a distance l. The pressure p_*, density ρ_*, and velocity $v_* = \sqrt{\gamma p_*/\rho_*}$ are prescribed on the source surface. The integration of equations for a steady-state, radial, supersonic, ideal gas flow under the above boundary conditions results in the following formulae for gas parameters at the point a distance r down the source centre

$$W = \left(\frac{r_*}{r}\right)^2 \left(\frac{2}{\gamma+1}\right)^{1/(\gamma-1)} \left(1-\frac{\gamma-1}{\gamma+1}W^2\right)^{-1/(\gamma-1)},$$
$$\frac{p}{p_*} = \left(\frac{r_*}{r}\right)^2 \frac{\gamma+1}{2W}\left(1-\frac{\gamma-1}{\gamma+1}W^2\right), \tag{1}$$
$$\frac{\rho}{\rho_*} = \left(\frac{r_*}{r}\right)^2 \frac{1}{W}.$$

Here $W = v/v_*$, v is the absolute value of the gas velocity vector. The geometric relations easily yield the formulae for the quantity r and for the angle of velocity vector inclination to the symmetry axis

$$r = [(l-R\cos\theta)^2 + R^2\sin^2\theta]^{1/2}$$
$$\varphi = \arctan\frac{R\sin\theta}{l-R\cos\theta}. \tag{2}$$

Relations (1) and (2) provide the dependence of the free-stream parameters on coordinates which is required to make shock-layer calculations.

Under the conditions considered the flow is accompanied by the formation of a detached shock wave in front of the body. The pressure p_* and density ρ_* on the source surface and the distance l are prescribed, according to equations (1) and (2), so that the required values of free-stream parameters would be ensured on the symmetry axis ahead of the bow shock wave. In this case the free-stream nonuniformity is governed only by the source-to-sphere radii ratio d.

Calculations of flow between the detached shock wave and the body surface were made by both the Euler and Navier–Stokes equations. The boundary conditions of the problem were formulated as follows. The symmetry relations were used on the stagnation line $\theta = 0$. On the downstream boundary of the calculation domain approximate conditions were assigned associated with the assumed sufficiently smooth variation of functions with respect to θ. As boundary conditions at the bow shock wave, the general Rankine–Hugoniot relations were used for the Euler equations and the generalized relations accounting for

NOMENCLATURE

a sphere radius
C_f skin-friction coefficient
C_f^m maximum value of skin-friction coefficient
C_H heat transfer coefficient at the forward stagnation point of sphere
d ratio of source and sphere radii
h specific enthalpy
k ratio between body surface temperature and free-stream stagnation temperature on symmetry axis
l distance between source and sphere centres
M Mach number
p pressure
Pr Prandtl number
q heat flux to body surface
r distance from source centre
R, θ spherical coordinates with the pole at sphere centre
Re Reynolds number
T temperature
u gas velocity vector component in θ direction.

Greek symbols
ρ density
γ ratio between gas specific heats
μ viscosity
φ angle of free-stream velocity vector inclination to symmetry axis
η similarity variable
ε detachment of bow shock wave from body surface
ω parameter of viscosity power dependence on temperature.

Subscripts
s gas parameters just behind bow shock wave on symmetry axis
0 gas parameters ahead of bow shock wave on symmetry axis
w body surface
* source parameters
∞ uniform free stream.

Superscripts
0 forward stagnation point
s sonic point on sphere surface in inviscid gas flow.

the viscosity and thermal conductivity effects for the Navier–Stokes equations. The solutions of Euler equations were then used to calculate the wall boundary layer. The body surface was assumed to be either adiabatic or having constant temperature. In all the cases the boundary conditions on the body surface were written without allowance for the velocity slip and temperature jump effects which are insignificant in the considered range of flow conditions [6].

Stationary solutions of the Euler and Navier–Stokes equations were found by the time-dependent technique with the aid of implicit finite-difference schemes [7–10]. The boundary-layer equations were integrated over the finite-difference scheme [11]. The accuracy of numerical solutions is 1–2% for the entire range of flow conditions considered. It was controlled by checking the fulfillment of the integral conservation laws, comparing the results obtained on different grids and with the use of different mathematical models, and also by comparing the results with experimental data.

As an example, Figs. 1 and 2 present some calculation results illustrating the effect of free-stream non-uniformity rarefaction on the shock-layer structure. Solid and dashed curves in Fig. 1 show the positions of shock waves and sonic lines obtained for a sphere in flows with different nonuniformity from the solution of Navier–Stokes equations. Figure 2 presents the longitudinal gas velocity component profiles in a shock-layer on the ray $\theta = 30°$. The dashed lines show the results of calculation of nonviscous flow. The solid and dash-dotted curves correspond to the solutions of Navier–Stokes equations for $Re_0 = 35500$ and 355.

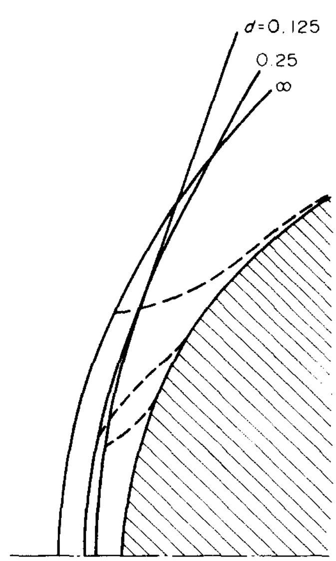

FIG. 1. Detached shock waves and sonic lines for the free stream of different nonuniformity: $M_0 = 6$, $Re_0 = 35500$, $k = 0.15$.

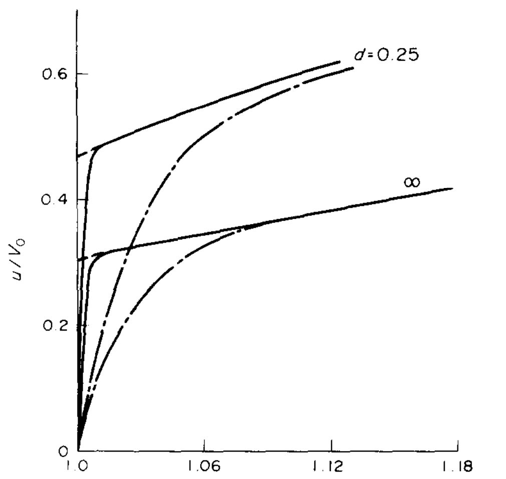

FIG. 2. Longitudinal gas velocity component profiles in a shock layer: $M_0 = 6$, $k = 0.15$.

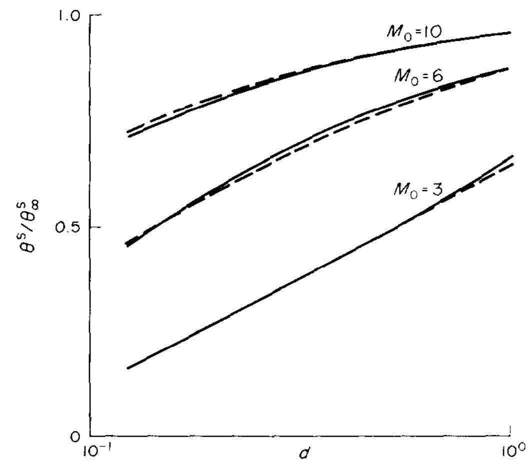

FIG. 3. Dependence of the sonic point position on a sphere on the nonuniformity parameter d.

UNIVERSAL RELATIONS

For the construction of the universal relations use was made of the results of calculations carried out for a diatomic gas with the specific heats ratio $\gamma = 1.4$, Prandtl number $Pr = 0.7$ and viscosity $\mu \sim \sqrt{T}$.

In earlier theoretical investigations of nonviscous gas flows past blunt bodies [2, 3] similarity was found in variation of the shock-layer parameters when angular coordinate was related to the value depending on free-stream nonuniformity. In the present work the similarity variable is used which was suggested in ref. [3]. The angular coordinate θ is related to its value at the sonic point on the sphere surface in a nonviscous gas flow. The calculations have shown that the use of such an independent variable brings together not only the distribution of pressure and shock-layer thickness but also the shear stress and heat flux distributions.

Figure 3 presents the dependence of the sonic point coordinate on a sphere in a nonviscous flow on the free-stream nonuniformity parameter d. The solid curves show the results of the author's calculations. The dashed curves are constructed from the approximate formula suggested in ref. [3]

$$\frac{\theta^s}{\theta^s_\infty} = \frac{1}{2}\left[1 + \frac{1}{K} - \sqrt{\left(\frac{1}{K} - 1\right)^2 + \frac{4}{Kl}}\right]. \quad (3)$$

Here $K = \varepsilon^0_\infty/(1+\varepsilon^0_\infty)$; the values of the shock wave detachment on the stagnation line ε^0_∞ and of the distance l are related to the sphere radius. It is seen that the sonic point coordinate for a nonuniform flow can be found with a good accuracy from formula (3).

Figures 4 and 5 present the distributions of the shock-layer thickness and also of pressure, heat flux and skin-friction coefficient on the sphere surface depending on the coordinate $\eta = \theta/\theta^s$. Most of these results were obtained from the solutions of nonviscous gas and boundary-layer equations. The solid curves correspond to a uniform free stream around a sphere at $M_0 = 6$, $k = 0.15$. It is seen that at $\eta \lesssim 1.5$ the distributions of the relative values of the shock-layer thickness, pressure, heat flux and skin-friction coefficient for nonuniform free stream are quite well described by the relations presented by the solid lines. At $\eta \gtrsim 1.5$ the departure from these relations and also the separation of the curves for different Mach numbers become noticeable. Corresponding segments of the distributions presented are described by the following approximate formulae

$$\frac{p_w}{p^0_w} = 0.76\eta^{-3.07}, \quad \eta \geqslant 1.5; \quad (4)$$

$$\frac{\varepsilon}{\varepsilon^0} = 0.62 \exp(0.82\eta), \quad \eta \gtrsim 1.6; \quad (5)$$

$$\frac{q}{q^0} = 2.65 \exp(-1.4\eta), \quad \eta \geqslant 1.3; \quad (6)$$

$$\frac{C_f}{C^m_f} = 3.01 \exp(-0.85\eta), \quad \eta \geqslant 1.65. \quad (7)$$

The results of calculations by these formulae are shown as dashed lines.

For one version of the flow parameters ($M_0 = 6$, $Re_0 = 177.5$, $k = 0.15$, $d = 0.25$), Figs. 4 and 5 present the results of the solution of the Navier–Stokes equations. It is seen that in the range of Reynolds numbers considered the effect of rarefaction on the universal distributions of flow characteristics falls within the scatter range due to the nonuniformity.

That the relations presented in Figs. 4 and 5 could be used, it is necessary to know the bow shock-wave detachment on the symmetry axis, the values of pressure and heat flux at the forward stagnation point and the maximum value of the skin-friction coefficient.

The pressure at the forward stagnation point of the sphere in a nonuniform free stream has the same value as in a uniform free stream. The calculated dependences

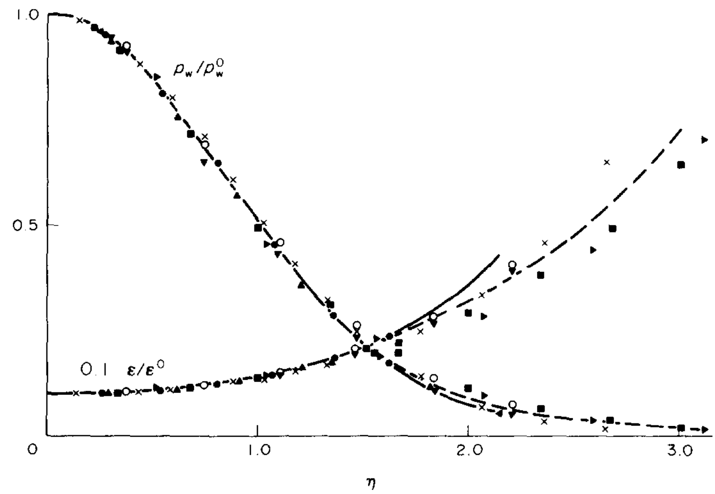

FIG. 4. Universal distributions of pressure and shock-layer thickness along the sphere surface: ●, $d = 1.00$; ▲, $d = 0.5$; ▼, $d = 0.25$, ▶, $d = 0.125$, $M_0 = 6$, $k = 0.15$; ○, $d = 0.25$, $M_0 = 6$, $Re_0 = 177.5$, $k = 0.15$; ■, $d = 0.25$, $M_0 = 3$, $k = 0.22$; ×, $d = 0.25$, $M_0 = 10$, $k = 0.06$.

of the values of ε^0, q^0, and C_f^m on the flow nonuniformity are depicted in Fig. 6. Solid curves 1–3 correspond to the solutions of nonviscous gas and boundary-layer equations for Mach numbers $M_0 = 3, 6, 10$. It is seen that the relations presented acquire a universal character with an increasing Mach number. Circles show the results of solution of the Navier–Stokes equations for $M_0 = 6$, $Re_0 = 355$. Comparison with the results obtained with the use of nonviscous gas and boundary-layer models shows that in the range of Reynolds numbers considered the rarefaction effect on the relative values of the shock-layer thickness, heat flux at the stagnation point and skin-friction coefficient is small.

Dashed lines in Fig. 6 correspond to the approximate relations [3, 4]

$$\frac{\varepsilon^0}{\varepsilon^0_\infty} = \frac{\theta^s}{\theta^s_\infty} \frac{1}{1+\varepsilon^0_\infty(1-\theta^s/\theta^s_\infty)}, \tag{8}$$

$$\frac{q^0}{q^0_\infty} = \sqrt{\frac{l}{l-1}}. \tag{9}$$

Formula (9) was derived for hypersonic free-stream velocities. However, even in this case its application leads to the heat flux values differing substantially from the results of numerical solutions.

With the use of all the above relations the determination of the parameters of nonuniform flow around a sphere reduces to the determination of their values for the case of uniform free stream.

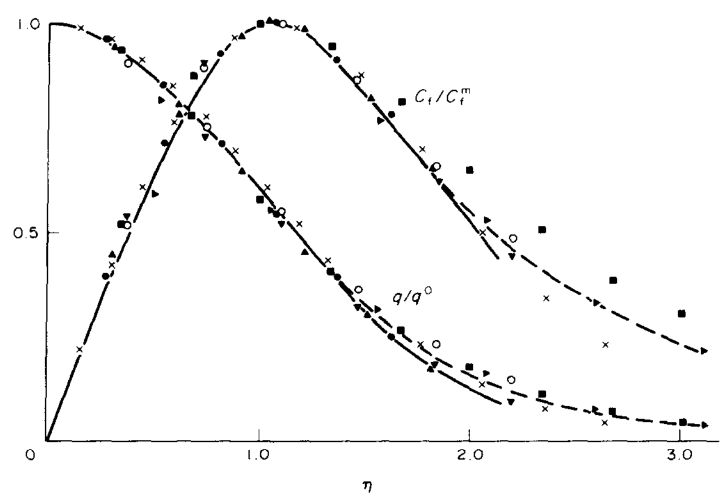

FIG. 5. Universal distributions of heat flux and skin-friction coefficient over the sphere surface: ●, $d = 1.00$, ▲, $d = 0.5$, ▼, $d = 0.25$, ▶, $d = 0.125$, $M_0 = 6$, $k = 0.15$; ○, $d = 0.25$, $M_0 = 6$, $Re_0 = 177.5$, $k = 0.15$; ■, $d = 0.25$, $M_0 = 3$, $k = 0.22$; ×, $d = 0.25$, $M_0 = 10$, $k = 0.06$.

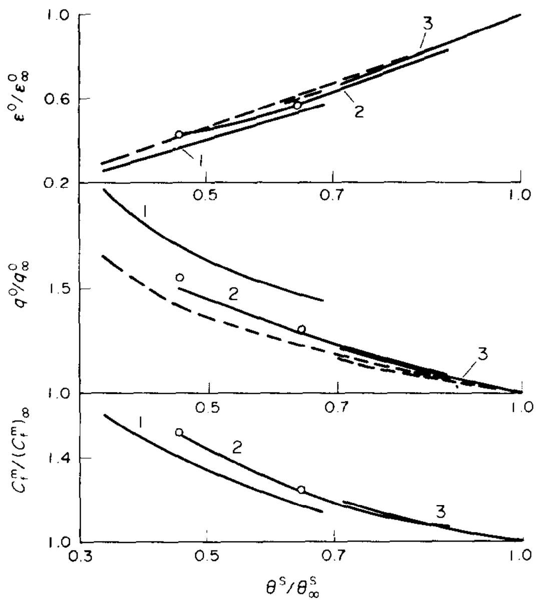

FIG. 6. Dependence of shock-wave detachment on the stagnation line, heat flux at the stagnation point and maximum value of skin-friction coefficient on the free-stream nonuniformity.

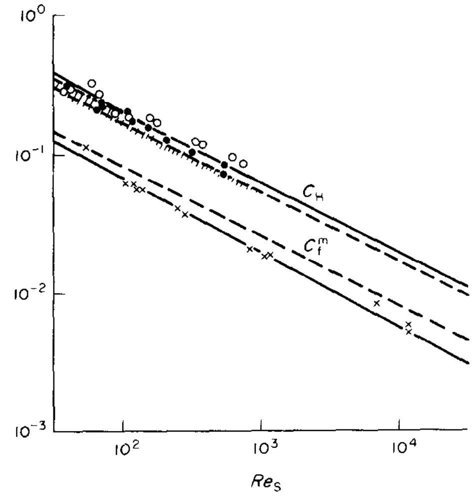

FIG. 8. Dependence of heat transfer coefficient at the forward stagnation point and of maximum skin-friction coefficient value on Reynolds number for a uniform free-stream flow around a sphere. Comparison with experimental data on heat transfer: ||| [12]; ○, [13]; ●, [14].

In the range of Reynolds numbers considered for this case the effect of rarefaction alters the pressure at the forward stagnation point by no more than several per cent [10]. The pressure is determined with this accuracy only by the gas specific heat ratio and free-stream Mach number.

The results for the shock-layer thickness, heat flux and shear stress for the case of uniform free stream are presented in Figs. 7 and 8. A convenient similarity criterion for the presentation of these results is the Reynolds number Re_s based on the gas parameters behind a normal shock wave. It is known that at large supersonic velocities the dependences of the flow characteristics on parameter Re_s vary very little with free-stream Mach number. When $\mu \sim T^\omega$, the relationship between the Reynolds numbers Re_s and Re_∞ is given by the formula

$$Re_s = \frac{\rho_s V_s a}{\mu_s} = Re_\infty \left[1 + \frac{2(\gamma-1)}{(\gamma+1)^2 M_\infty^2} \times (M_\infty^2 - 1)(1+\gamma M_\infty^2) \right]^{-\omega}. \quad (10)$$

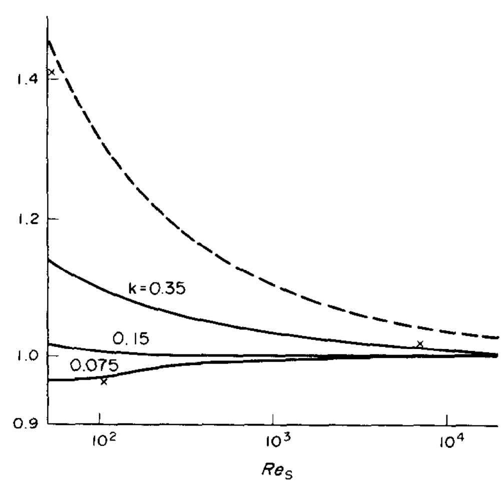

FIG. 7. Dependence of the shock-wave detachment on the symmetry axis on Reynolds number for a uniform free-stream flow around a sphere.

In Fig. 7 the solid curves depict a variation of the shock-wave detachment on the symmetry axis at different values of the wall temperature factor k. The dashed curve corresponds to the adiabatic wall case. The detachment is referred to its value for a nonviscous gas. These results are obtained from the solution of the Navier–Stokes equations at the Mach number $M_\infty = 6$. They demonstrate rather a substantial effect of the wall temperature factor on the shock-layer thickness at small Reynolds numbers. At the same time these relations vary little with a change in the Mach number. To illustrate this fact, Fig. 7 gives the results of calculations for $M_\infty = 13.4$, $k = 0.073$; $M_\infty = 2$, $k = 0.35$, and $M_\infty = 3.74$ in the case of an adiabatic wall. All these results are shown by the symbol ×.

Figure 8 presents the dependence of the stagnation point heat transfer parameter, $C_H = q^0/\rho_\infty V_\infty(h^* - h_w)$, and of the maximum skin-friction coefficient value on the sphere surface, C^m_f, on the Reynolds number Re_s. Here h^* is the free-stream stagnation enthalpy. The skin-friction coefficient is defined as the ratio of shear stress on the body surface to the quantity $\rho_\infty V_\infty^2$.

For heat transfer parameter the solid curve corresponds to calculations for $\mu \sim \sqrt{T}$, the dashed curve, to calculations for $\mu \sim T$. These relations describe, accurate to within 3%, the results obtained from the solution of Navier–Stokes equations at $M_\infty = 6$ and $0.075 \leqslant k \leqslant 0.35$. The dashed-dotted line presents the results of boundary-layer calculation for $M_\infty = 6$, $k = 0.15$, $\mu \sim \sqrt{T}$. The relations for the heat transfer parameter agree well with the experimental data [12–14] obtained within the Mach number range $2 \leqslant M_\infty \leqslant 18$.

The solid curve for the quantity C_f^m in Fig. 8 corresponds to the flow around a cooled sphere at $k = 0.15$, the dashed curve, to the adiabatic wall case. In both of the cases it was assumed that $M_\infty = 6$ and $\mu \sim \sqrt{T}$. The calculations have shown that within the range of the wall temperature factor $0.075 \leqslant k \leqslant 0.35$ the function $C_f^m(Re_s)$ is described accurate to 5% by the curve corresponding to $k = 0.15$. On an adiabatic wall the skin-friction coefficient is higher than on a cooled one, which corresponds to a higher viscosity value on the body surface. A slower increase of skin-friction coefficient on the adiabatic wall than on a cooled one with a decrease in the number Re_s is due to a different effect of rarefaction on the shock-layer thickness in these cases (see Fig. 7).

The symbol × in Fig. 8 denotes the values of the skin-friction coefficient calculated for cooled and adiabatic wall cases in the range of free-stream Mach numbers $2 \leqslant M_\infty \leqslant 18$. As was expected, the largest deviation from the universal relations is observed at $M_\infty = 2$. It should be noted that under the flow conditions considered the functions $C_H(Re_s)$ and $C_f^m(Re_s)$, plotted on a logarithmic scale, differ insignificantly from the linear boundary-layer relations.

CONCLUDING REMARKS

The problem of flow from a supersonic source past a spherical bluntness is considered. The distributions over the sphere surface of the relative values of shock-layer thickness, pressure, heat flux and skin-friction coefficient are represented in the form of universal functions weakly dependent on the Mach and Reynolds numbers, wall temperature factor and free-stream nonuniformity.

As formulae and graphs the relations are presented the use of which, to approximately determine the above quantities at any point on the front part of the sphere surface, requires only the information about the characteristics of ideal gas flow around a sphere immersed in a uniform free stream.

The results presented are based on numerical solutions of the problem for a gas with the specific heats ratio $\gamma = 1.4$. However, the similarity properties are valid also for other gases and gas mixtures. This is confirmed by the present author's calculations for a monoatomic gas with $\gamma = 1.67$ and with the results [3] for a nonviscous equilibrium air.

REFERENCES

1. N. E. Khramov, Calculation of nonuniform gas flow around a sphere, *Prikl. Mat. Mekh.* **29**, 175–177 (1965).
2. V. V. Lunyov and N. E. Khramov, Flow in the vicinity of the blunt body stagnation point in a divergent hypersonic stream, *Izv. Akad. Nauk SSSR, Mekh. Zhid. Gaza* **3**, 102–105 (1970).
3. E. G. Shapiro, On certain similarity properties of supersonic uniform and nonuniform gas flows around a sphere, *Izv. Akad. Nauk SSSR, Mekh. Zhid. Gaza* **1**, 82–85 (1975).
4. I. G. Eremeitsev and N. N. Pilyuguin, Convective heating of a blunt body in a hypersonic nonuniform gas flow, *Izv. Akad. Nauk SSSR, Mekh. Zhid. Gaza* **4**, 127–133 (1981).
5. Yu. P. Golovachov and N. V. Leontieva, Viscous shock layer near the surface of a blunt body in a divergent supersonic flow, *Izv. Akad. Nauk SSSR, Mekh. Zhid. Gaza* **3**, 176–179 (1983).
6. A. C. Jain and V. Adimurthy, Hypersonic merged stagnation shock layers, *AIAA Jl* **12**, 342–354 (1974).
7. A. N. Lyubimov and V. V. Rusanov, *Gas Flow Near Blunt Bodies*, Vol. 1. Izd. Nauka, Moscow (1970).
8. Yu. P. Golovachov and F. D. Popov, Calculation of viscous gas supersonic flow past blunt bodies at high Reynolds numbers, *Zh. Vychisl. Mat. mat. Fiz.* **12**, 1292–1303 (1972).
9. Yu. P. Golovachov, A. M. Kuzmin and F. D. Popov, Concerning the calculation of supersonic flow around blunt bodies with the use of full and simplified Navier–Stokes equations, *Zh. Vychisl. Mat. mat. Fiz.* **13**, 1021–1028 (1973).
10. O. M. Belotserkovsky, Yu. P. Golovachov, V. G. Grudnitsky, Yu. M. Davydov, V. K. Dushin, Yu. P. Lunkin, K. M. Magomedov, V. K. Molodtsov, F. D. Popov, A. I. Tolstykh, V. N. Fomin and A. C. Kholodov, *Numerical Investigation of Modern Gasdynamic Problems.* Izd. Nauka, Moscow (1974).
11. A. P. Byrkin and V. V. Shchennikov, On one numerical method of the laminar boundary layer calculation, *Zh. Vychisl. Mat. mat. Fiz.* **10**, 124–131 (1970).
12. R. S. Hickman and W. H. Giedt, Heat transfer to a hemisphere–cylinder at low Reynolds number, *AIAA Jl* **1**, 665–672 (1963).
13. M. R. Wilson and C. E. Wittliff, Low density stagnation point heat transfer measurements in hypersonic shock tunnel, *AIAA Jl* **32**, 275–276 (1962).
14. V. N. Gusev and Yu. V. Nikolsky, Experimental investigation of heat transfer at the sphere stagnation point in a supersonic rarefied gas flow, *Uchyon. Zap. TsAGI* **8**, 122–125 (1971).

PROPRIETES DE SIMILITUDE DANS LE PROBLEME DE L'ECOULEMENT ISSU D'UNE SOURCE SUPERSONIQUE SUR UN NEZ SPHERIQUE

Résumé—On considère l'écoulement permanent de gaz parfait issu d'une source sphérique supersonique et passant sur un nez sphérique. Des solutions numériques sont données pour les équations des gaz non visqueux, de couche limite et de Navier–Stokes. Des relations universelles pour le transfert thermique et le frottement sont construites et elles s'appliquent à un large domaine de nombres de Mach et de Reynolds pour différentes uniformités d'écoulements libres.

ÄHNLICHKEITSEIGENSCHAFTEN BEIM PROBLEM DER ÜBERSCHALLSTRÖMUNG UM KUGELFÖRMIG ABGESTUMPFTE KÖRPER

Zusammenfassung—Die stationäre ideale Gasströmung von einer kugelförmigen Überschallquelle um kugelförmig abgestumpfte Körper wurde betrachtet. Basierend auf numerischen Lösungen der nichtviskosen Gasgleichungen, Grenzschicht- und Navier–Stokes-Gleichungen, wurden allgemeine Beziehungen für die Wärmeübertragung und die Widerstands-Parameter entwickelt, die in einem großen Bereich von Mach- und Reynolds-Zahl für unterschiedlich gleichförmige freie Strömungen angewandt werden können.

СВОЙСТВА ПОДОБИЯ В ЗАДАЧЕ ОБТЕКАНИЯ СФЕРИЧЕСКОГО ЗАТУПЛЕНИЯ ПОТОКОМ ОТ СФЕРХЗВУКОВОГО ИСТОЧНИКА

Аннотация—Рассматривается стационарное обтекание сферического затупления потоком совершенного газа от сферхзвукового сферического источника. На основе численных решений уравнений невязкого газа, пограничного слоя и уравнений Навье–Стокса построены универсальные зависимости для параметров теплообмена и сопротивления, применимые в широком диапазоне чисел Маха и Рейнольдса при различной неравномерности набегающего потока.